

# Implementing initial state radiation for lepton induced processes in AMEGIC++

---

**A. Schälicke<sup>a,b</sup>, F. Krauss<sup>b</sup>, R. Kuhn<sup>a</sup>, and G. Soff<sup>a</sup>**

<sup>a</sup>*Institut für Theoretische Physik, TU Dresden, 01062 Dresden, Germany*

<sup>b</sup>*Cavendish Laboratory, University of Cambridge, Cambridge CB3 0HE, U.K.*

*E-mail:* schalicke@hep.phy.cam.ac.uk, krauss@hep.phy.cam.ac.uk,  
kuhn@theory.phy.tu-dresden.de

**ABSTRACT:** We have implemented the method of Yennie, Frautschi, and Suura up to first order in  $\alpha$  for the simulation of QED Initial State Radiation in lepton induced processes in AMEGIC++. We consider  $s$ -channel processes via the exchange of scalar or vector resonances at electron and muon colliders.

**KEYWORDS:** Standard Model, Supersymmetric Standard Model, Higgs Physics, Electromagnetic Processes and Properties.

---

## Contents

<b>1. Introduction</b>	<b>1</b>
<b>2. Method</b>	<b>3</b>
<b>3. Implementation</b>	<b>8</b>
<b>4. Results</b>	<b>9</b>
<b>5. Conclusion and Outlook</b>	<b>13</b>
<b>A. The MC algorithm</b>	<b>15</b>
<b>B. Program Parameters</b>	<b>17</b>

---

## 1. Introduction

Initial State Radiation (ISR) is the most important QED correction to the Born cross section. For instance, in the case of electron positron annihilations at energies beyond the  $Z$ -threshold it leads to the so-called radiative return causing a hugely increased cross section. There, via multiple emission of photons, the electron positron pair tends to reside on the  $Z$ -resonance (returning on it) picking up the propagator in its resonance region. In this way, the correction term becomes several times as large as the Born term at the initial center of mass energy. Evidently, the effect of ISR is of great significance for the interpretation of experimental results. However, since initial state photons tend to be collinear and soft they easily escape detection. In the detector, they tend to leave only imprints by a reduced overall energy and some netto transverse momentum and – possibly – by a boost of the visible final state along the beam axis. Due to this rather indirect method of measuring it, the precise simulation of ISR is crucial for most experimental analyses.

Several strategies exist for this task:

1. The structure function approach

The idea behind this approach is to simulate ISR by a probability density to find an electron with reduced momentum inside an incoming electron. Accordingly, the missing momentum is then attributed to photon radiation. That way the total cross section  $\sigma_{\text{tot}}$  including ISR is defined as the leading order cross section  $\sigma_{\text{B}}$  convoluted with two structure functions  $\Gamma_{ee}$ :

$$\sigma_{\text{tot}} = \int dx_1 dx_2 \Gamma_{ee}(x_1, s) \Gamma_{ee}(x_2, s) \sigma_{\text{B}}(x_1 x_2 s) . \quad (1.1)$$

Within the structure functions logarithmically enhanced contributions are exponentiated and thus re-summed to all orders with additional terms covering non-factorisable QED effects up to a finite order  $\alpha^n$ . Additionally, terms describing weak and strong effects can be taken into account. However, since the structure function is integrated over all photon energies and transverse momenta, it is limited to situations in which only the overall effects of energy reduction and longitudinal boost via ISR are of interest. Arbitrary phase space cuts are difficult to implement. Specific photonic observables like for instance the number of photons above some energy threshold or their transverse momenta are beyond the reach of this approach.

## 2. The parton shower approach

In this approach, the electron radiation is followed step by step from the comparably low scales of the order of the electron mass connected to the incoming electrons to the high energy scale of the actual hard process. After setting up an electron distribution function at the initial scale, any individual photon emission is governed by the well-known splitting function

$$P_{ee}(z) = \frac{\alpha}{2\pi} \frac{1+z^2}{1-z} \quad (1.2)$$

leading to a Dokshitzer–Gribov–Lipatov–Altarelli–Parisi (DGLAP) evolution equation for the structure function. Technically, the original structure function is being reproduced statistically at each scale via backward evolution and re-weighting, where the analytic integration is replaced by Monte Carlo integration. Apparently, photons are generated explicitly which allows for instance the application of arbitrary phase space cuts. However, one of the weaknesses of this approach is that it re-sums only the logarithmic enhanced contributions in the DGLAP equation. Even though the radiation of the hardest photon can be corrected with the first order matrix element, it is not clear how to systematically improve to higher perturbative order, i.e. how to make sure that matrix element expressions for the emission of additional photons are recovered for arbitrary processes and arbitrary numbers of photons.

## 3. The approach by Yennie, Frautschi and Suura (YFS) [1]

Within this approach the explicit generation of photons can be corrected systematically to all orders in the coupling constant. The basic idea here is to introduce some arbitrary infrared cut-off on the photon energies and treat low energy real photons as “un-resolvable”. Their respective contribution will cancel the emerging virtual infrared divergences to all orders leading to finite factorisable terms which can be exponentiated. In this framework correction terms for harder photons can be easily introduced. Since this is the approach we are going to follow we postpone a more thorough discussion.

In this paper we want to give a description of the YFS method implemented in **AMEGIC++** [2]. The outline is as follows: In section 2, after briefly reviewing the YFS approach and a short introduction to the nomenclature, we will introduce our new approach to calculate

matrix element corrections, where we make use of the ability of **AMEGIC++** to calculate (almost) arbitrary tree level matrix elements automatically. In fact, it can be anticipated that our method might allow for the construction of a more generic simulation code for QED initial state radiation in arbitrary processes in the near future. In section 3 we will discuss the actual implementation of our approach and the interplay of ISR with the calculations of matrix elements and cross sections. We justify our method in section 4 by confronting our results for the radiative return to the  $Z$ -pole with experimental data from the LEP experiment. The generality of our program is illustrated by the application to the  $s$ -channel production of Higgs bosons at a possible muon collider. We will conclude with summarizing remarks.

## 2. Method

In this section we want to discuss our new method to include the effect of exact matrix elements in the generation process of initial state photons along the lines of the YFS approach. We will begin with a mini-review of this method suitable for Monte Carlo implementation.

### Mini-review of the YFS approach

The idea underlying the YFS approach is to separate the phase space for the emission of real photons into two regions via a cut-off  $\epsilon$  on the energy fractions, such that photons are coined infrared if their energies  $\omega_\gamma < \epsilon E_{\text{beam}}$ . The contribution of these infrared photons is then used to cancel the virtual infrared divergences order by order in  $\alpha$ . The remainders of this procedure factorize and can be exponentiated into an universal factor, the YFS form factor:

$$\begin{aligned} F^{\text{YFS}}(\epsilon) &= \exp \left[ 2\alpha(B + \tilde{B}) \right] \\ &= \exp \left[ \frac{\alpha}{\pi} \left( \frac{1}{2} \ln \frac{s}{m^2} - 1 + \frac{\pi^2}{3} \right) + \frac{2\alpha}{\pi} \left( \ln \frac{s}{m^2} - 1 \right) \ln \epsilon \right] . \end{aligned} \quad (2.1)$$

The virtual part is given by

$$\alpha B = \int \frac{d^D k}{(2\pi)^D} \frac{1}{k^2} S(k) \quad (2.2)$$

whereas the real contribution reads

$$\alpha \tilde{B} = \int_{\omega < \epsilon E} \frac{d^{D-1} k}{(2\pi)^{D-1} 2\omega} \tilde{S}(k) . \quad (2.3)$$

The functions  $S(k)$  and  $\tilde{S}(k)$  denote the well known universal factorizing “radiation factors” or “eikonal factors” for virtual and real photons for a pair of two external charged lines with four-momenta  $p_1$  and  $p_2$

$$\begin{aligned} S(k) &= -\frac{\alpha}{8\pi} \left[ \frac{2p_1^\mu - k^\mu}{k^2 - 2kp_1} - \frac{2p_2^\mu - k^\mu}{k^2 - 2kp_2} \right]^2 , \\ \tilde{S}(k) &= \frac{\alpha}{4\pi} \left[ \frac{p_2^\mu}{kp_2} - \frac{p_1^\mu}{kp_1} \right]^2 . \end{aligned} \quad (2.4)$$

The emission of the visible real photons can then be corrected systematically to all orders in  $\alpha$  to reproduce exact results as given by the corresponding matrix elements. To be more specific, let us consider as an example  $2 \rightarrow 2$  processes of the type  $l^+(p_1) l^-(p_2) \rightarrow f(q_1) \bar{f}(q_2)$ , where the  $p_i$  and  $q_j$  label the four-momenta of the external particles. The total cross section including arbitrary numbers of real or virtual photons can be written as

$$\sigma = F^{\text{YFS}}(\varepsilon) \int \frac{d^3 \vec{q}_1}{q_1^0} \frac{d^3 \vec{q}_2}{q_2^0} \sum_{n=0}^{\infty} \left\{ \frac{1}{n!} \left[ \prod_{i=1}^n \frac{d^3 \vec{k}_i}{k_i^0} \tilde{S}(p_1, p_2, k_i) \Theta \left( \frac{2k_i^0}{\sqrt{s}} - \varepsilon \right) \right] \right. \\ \delta^4 \left( p_1 + p_2 - q_1 - q_2 - \sum_{i=1}^n k_i \right) \\ \left. \left( \beta_0 + \sum_{j=1}^n \frac{\beta_1(k_j)}{\tilde{S}(k_j)} + \sum_{j,l=1, j \neq l}^n \frac{\beta_2(k_j, k_l)}{\tilde{S}(k_j) \tilde{S}(k_l)} + \dots \right) \right\}. \quad (2.5)$$

The YFS form factor  $F^{\text{YFS}}(\varepsilon)$  covers the contribution of factorizing soft real and virtual photons to all orders. The integral over the phase space of the final state particles consists of the integral over the two outgoing momenta  $q_1$  and  $q_2$  plus a sum over all possible numbers of photons  $k_i$  with energy fractions above the resolution threshold  $\epsilon$ . This constraint is reflected in the  $\Theta$ -functions. The conservation of total four-momentum is enforced by the  $\delta$ -function in the second line. Finally, the last line includes the matrix element corrections. The  $\beta_n$  denote infrared safe combinations of cross sections and eikonal factors with  $n$  additional real photons as well as all finite contributions of any number of virtual photon loops. In practice, the order of virtual contributions is limited. In  $\beta_n^{(l)}$  the superscript  $l$  denotes the total number of virtual and real photons taken into account, i.e. the order of perturbation theory. From there we can read off the number of virtual photons, given by  $(l - n)$ .

For a treatment exact up to first order  $\alpha$ , it is sufficient to determine  $\beta_0^{(0)}$ ,  $\beta_0^{(1)}$  and  $\beta_1^{(1)}$ , i.e. the cross sections for  $l^+(p_1) l^-(p_2) \rightarrow f(q_1) \bar{f}(q_2)$  up to one loop and for  $l^+(p_1) l^-(p_2) \rightarrow f(q_1) \bar{f}(q_2) \gamma(k_i)$  at the tree level. They are defined as

$$\beta_0^{(0)} = \rho_0^{(0)}, \quad \beta_0^{(1)} = \rho_0^{(1)}, \\ \beta_1^{(1)}(k_i) = \rho_1^{(1)}(k_i) - \tilde{S}(k_i) \beta_0^{(0)}. \quad (2.6)$$

The  $\rho_n^{(l)}$  are the fully differential cross sections for the hard process  $l^+(p_1) l^-(p_2) \rightarrow f(q_1) \bar{f}(q_2)$  with  $n$  real photons added and up to  $l$ th order in  $\alpha$ , and  $\tilde{S}$  denotes the eikonal factor as defined in Eq.(2.4).

Analyzing the master equation, Eq.(2.5), we realize that

1. the number of photons that are explicitly produced is not constrained,
2. the resolved photons are allowed to have transverse momentum,
3. the cross section is independent of  $\epsilon$  (in fact, only the number of explicitly produced photons depends on the resolution scale), and

4. that in contrast to the parton shower approach any photon emission is corrected by the appropriate matrix element(s) to the chosen order in  $\alpha$  including interference effects in multi photon final states.

### The MC algorithm

A Monte Carlo implementation for the YFS approach outlined above was described in [3] for the first time. The proposed procedure there was

1. to chose the c.m. energy with the form factor  $F^{\text{YFS}}$ ,
2. to determine the number of resolvable photons,
3. to supply each of the photons with a four-momentum  $k$  according to the eikonal factor  $\tilde{S}(k)$ ,
4. to reject all momenta outside their kinematical limits, and
5. to correct the configuration chosen with an additional weight stemming from the exact matrix element.

A more detailed description of the Monte Carlo steps can be found in Appendix A.

### Implementing matrix element corrections

The corrections on the photon distributions and the cross sections due to exact matrix elements can be read off from Eq.(2.5). Up to first order in  $\alpha$  the corresponding weight reads:

$$w_{\text{ME}} = \frac{1}{\sigma_B(s')} \left\{ \beta_0^{(1)}(p_i, q_j) + \sum_{n=1}^{N_\gamma} \frac{\beta_1^{(1)}(p_i, q_j, k_n)}{\tilde{S}(p_i, k_n)} \right\}, \quad (2.7)$$

where again the  $p_i$  are the incoming momenta, the  $q_j$  are the outgoing momenta and the  $k_n$  are the momenta of the explicitly generated photons. In the following we will again restrict ourselves to the description of the process  $e^+e^- \rightarrow f\bar{f}$ , i.e. a process with two incoming and two outgoing momenta only. However, the extension to more final state particle is straightforward.

An implementation of this weight might seem trivial, however, one serious question remains: How do we calculate matrix elements in situations, where the number of generated photons exceeds the number incorporated in the matrix element? Matrix elements are only unambiguously defined if all incorporated momenta comply with four-momentum conservation. This leads to a problem in cases when some of the generated photon momenta are omitted.

In general, it is solved by applying an unique description of how to evaluate  $\beta$  functions. Two approaches have been developed in the past to deal with this situation, namely the projection method [3] and the extrapolation method [4]. In the following we will briefly discuss both methods in order to point out their advantages and disadvantages. Our own solution will be presented afterwards.

The projection method defines for each  $\beta_n$  function a mapping of the four-momenta from the full phase space with  $N_\gamma$  photons to the restricted phase space with only  $n$  photons. Therefore,  $N_\gamma - n$  momenta are completely discarded. The four-momenta of the remaining particles are transformed such that they again comply with four-momentum conservation. In general, this is achieved by a sequence of scalings and boosts applied in individual combinations on the incoming and outgoing particles. For instance, for the leading order term  $\beta_0$  the projected momenta  $p'_i, q'_j$  are obtained by boosting the incoming momenta  $p_1$  and  $p_2$  into their common c.m. frame and scaling them to fulfill the condition  $(p'_1 + p'_2)^2 = (q_1 + q_2)^2 = s'$ . The outgoing momenta  $q'_1$  and  $q'_2$  are thus defined by boosting the original  $q_j$  into their common c.m. frame. A projection for higher order corrections is more involved and will be discussed at the end of this section in the framework of our new approach.

The extrapolation method, on the other hand, defines the matrix element in any phase space with additional photons, i.e. the momenta are kept untouched but the matrix element is rewritten in a suitable set of variables like e.g. angles and energies. Obviously, there is no universal way to construct this transformation and therefore this has to be done for each matrix element separately.

As an example we briefly review the corresponding algorithm in the program KoralZ, that is dealing with processes of the type  $e^+e^- \rightarrow f\bar{f}$  with  $f \neq e^-$ . The leading order term  $\beta_0$  is written as

$$\beta_0(p_i, q_j; k_1, \dots, k_{N_\gamma}) = \frac{1}{2} \left[ \frac{d\sigma_0}{d\Omega}(s', \cos \vartheta_1) + \frac{d\sigma_0}{d\Omega}(s', \cos \vartheta_2) \right], \quad (2.8)$$

where

$$\cos \vartheta_1 = \frac{\vec{p}_1 \vec{q}_1}{|\vec{p}_1| |\vec{q}_1|} = - \frac{\vec{p}_1 \vec{q}_2}{|\vec{p}_1| |\vec{q}_2|} \quad (2.9)$$

and

$$\cos \vartheta_2 = \frac{\vec{p}_2 \vec{q}_2}{|\vec{p}_2| |\vec{q}_2|} = - \frac{\vec{p}_2 \vec{q}_1}{|\vec{p}_2| |\vec{q}_1|} \quad (2.10)$$

are the angles between equal and opposite charged particles, respectively. In the presence of additional photons these angles differ, but  $\beta_0$  is well calculable for any number of photons, since the variables  $s' = (q_1 + q_2)^2$ ,  $\cos \vartheta_1$ , and  $\cos \vartheta_2$  are defined in all cases. For the calculation of  $\beta_1$  the variable  $s = (p_1 + p_2)^2$  and the polar angle of the photon  $\cos \vartheta_\gamma$  are used in addition to  $\cos \vartheta_1$ ,  $\cos \vartheta_2$  and  $s'$ .

However, any approach to define matrix element corrections has to comply with two conditions:

- First, the method has to guarantee that the original result is retained in case the neglected “spectator” photons have total zero four-momentum. In particular, this must hold true in the case of zero spectators.
- Second, the procedure should not give rise to new large logarithms at any order beyond the perturbative order up to which the weight is defined.

At this stage we would like to present a new method to define the  $\beta$  functions. We aim at a general approach that takes full advantage of the automatic calculation of tree-level

matrix elements in **AMEGIC++**. We do not want to interfere with the automatic calculation as such, which relies on the construction of four-momenta and their explicit conservation. Hence, the method of choice is rather a realization of the projection method. Remember that the first order infrared finite correction term is

$$\beta_1(p_i, q_j, k_n) = \rho_1^{(1)}(p_i, q_j, k_n) - \tilde{S}(p_i, k_n) \beta_0^{(0)}(p_i, q_j) . \quad (2.11)$$

For this correction term the projection method is well defined as long as there is exactly one additional photon. Then we can apply the PM as introduced for the leading order term  $\beta_0$  by redefining  $\beta_1$  as

$$\beta_1(p_i, q_j, k_n) = \rho_1^{(1)}(p_i, q_j, k_n) - \tilde{S}(p_i, k_n) \beta_0^{(0)}(p'_i, q'_j) . \quad (2.12)$$

For more than one photon the arguments of the differential cross section  $\rho_1^{(1)}$  have to be projected as well. Naively, one might want to apply the same technique as for  $\beta_0$  with the photon  $k_i$  included in the outgoing momenta, but it turns out that this is not sufficient to describe events with additional hard photons.

Our solution to this problem is the following:

1. The second term, consisting of the eikonal factor multiplied with the Born term cross section is still treated as described above. Here, we observe that
  - the scale of the evaluation of the eikonal is  $s$ , since it is evaluated with the original vectors  $p_1$  and  $p_2$ . This means that the effect of all other photons is ignored which yields the correct behavior in order to cancel the eikonal factors in the YFS exponent.
  - The scale of the Born cross section, i.e. the scale of the  $s$ -channel propagator, is  $s'$ .
2. In the first term we have to obtain a similar structure. This is achieved by the following steps:
  - To calculate the photon part at the scale  $s$ , it is necessary to leave the incoming momenta as well as the photon momentum untouched, but the outgoing momenta have to be modified. The new momenta  $\hat{q}_1$  and  $\hat{q}_2$  are fixed by the constraint

$$p_1 + p_2 = \hat{q}_1 + \hat{q}_2 + k_n .$$

Thus, the differential cross section with one photon is given by

$$\rho_1^{(1)}(p_1, p_2, \hat{q}_1, \hat{q}_2, k_n) . \quad (2.13)$$

- In the previous step, the scale of the  $s$ -channel propagator has been changed to  $\hat{s} = (\hat{q}_1 + \hat{q}_2)^2$  which can modify the cross section quite drastically. We cure this by a correction factor

$$C = \frac{\beta_0(p'_1, p'_2, q'_1, q'_2)}{\beta_0(\hat{p}_1, \hat{p}_2, \hat{q}_1, \hat{q}_2)} . \quad (2.14)$$



Thus, the right peak structure is restored. The new incoming momenta are naturally defined via  $\hat{s} = (\hat{p}_1 + \hat{p}_2)^2$ .

Altogether,  $\beta_1$  is defined as

$$\beta_1(p_i, q_j, k_n) = \frac{\beta_0(p'_i, q'_j)}{\beta_0(\hat{q}_i, \hat{q}_j)} \rho_1(p_i, \hat{q}_j, k_n) - \tilde{S}(p_i, k_n) \beta_0(p'_i, q'_j) . \quad (2.15)$$

### 3. Implementation

In this section we want to discuss some aspects of the interplay of **AMEGIC++** with its ISR module. A more thorough description of **AMEGIC++** is available in the manual [2], here we just list the basic steps to calculate cross sections:

1. As a first step, **AMEGIC++** sets up the model in which the calculation is going to take place. This includes the definition of particles, the initialization of Feynman rules in terms of vertices and – possibly – the determination of the widths of unstable particles. This last step already relies on the construction and evaluation of corresponding Feynman diagrams and their integration.
2. The construction of Feynman diagrams is performed in three steps:
  - The construction of “empty” topologies, i.e. without the specification of lines and vertices,
  - their mapping on “filled” Feynman diagrams with specified propagators and vertices,
  - and, finally, their translation into helicity amplitudes which can be stored in library files.
3. The integration of the diagrams is done with help of an adaptive multichannel method [5]. The channels are constructed by inspection of the kinematical structure of corresponding Feynman diagrams.

Implementing ISR in the framework of YFS affects the last two steps. First, **AMEGIC++** has to provide one additional matrix element to calculate the real photon matrix element corrections. The second step is therefore extended as follows:

- An “ISR–Photon” is defined, i.e. an additional particle type is introduced, with all properties of an ordinary photon but exclusively coupling to the charged particles in the initial state.
- One “ISR–Photon” is added to the list of outgoing particles. Correspondingly, “empty” topologies with one additional leg are constructed.
- The Feynman diagrams for this additional process are generated and translated into helicity amplitudes as pointed out above.

During the integration, step 3, the following changes take place:

- The reduced c.m. energy  $\sqrt{s'}$  is determined, and a number of ISR photons is generated along the lines of the algorithm in Appendix A. With this energy a set of incoming momenta is defined in their c.m. frame.
- The momenta of the final state are generated and the leading order cross section is calculated with a multichannel method. So far the effect of ISR is only manifest by the reduced c.m. energy.
- The ISR weight is calculated using the generated final state momenta. Therefore, the matrix element prepared in step 2 with one additional photon as well as the Born matrix element are used according to our method introduced in section 2. The obtained weight is combined with the phase space weight.
- Finally, a boost of all incoming and outgoing momenta is performed in a way that all momenta, i.e. including the ISR photons, comply with four-momentum conservation. Note that this step does not modify the result of the integrated cross section but it is mandatory, when AMEGIC++ is used inside a Monte Carlo generator.

## 4. Results

To demonstrate the quality of our approach we will discuss two examples:

- Processes of the type  $e^+e^- \rightarrow \gamma^*, Z^* \rightarrow f\bar{f}$  at LEP2 energies including comparison with both experimental data and other generators (KoralZ).
- Processes of the type  $\mu^+\mu^- \rightarrow \gamma^*, Z^*, h^* \rightarrow f\bar{f}$  at higher energies including the effect of propagating Higgs bosons, both from the Standard Model and its minimal supersymmetric extension (MSSM).

$$e^+e^- \rightarrow f\bar{f}$$

The effect of ISR on processes of the type  $e^+e^- \rightarrow f\bar{f}$  at LEP2 energies is tremendous. Due to the “Radiative Return” huge numbers of events actually reside on the  $Z^0$  resonance instead of the beam energy.

The effect is twofold: First, the visible energy in the detector tends to be reduced to energies of the order of the  $Z$  mass accompanied by an increase of the total cross section. Secondly, the forward-backward asymmetry due to the axial coupling of the  $Z$  boson tends to be shifted correspondingly.

We will highlight this effect in a series of figures. Fig.1 exhibits the total cross section for  $e^+e^- \rightarrow \mu^+\mu^-(\gamma)$  in comparison with data from the DELPHI collaboration [6]. Fig. 2 depicts the combined forward-backward asymmetry in  $\mu$  and  $\tau$  pair production at LEP2 compared to data taken by OPAL [7]. Finally, Fig. 3 shows the differential cross section with respect to the cosine of the angle between equally charged incoming and outgoing leptons compared to data from L3 [9]. To guide the eye, we have included the uncorrected Born level prediction with a black line in the first two figures.

In all three cases different cuts on  $s'$  have been applied, and in all cases the agreement of our generator with data is very good. Note that we did not take into account any FSR effects.

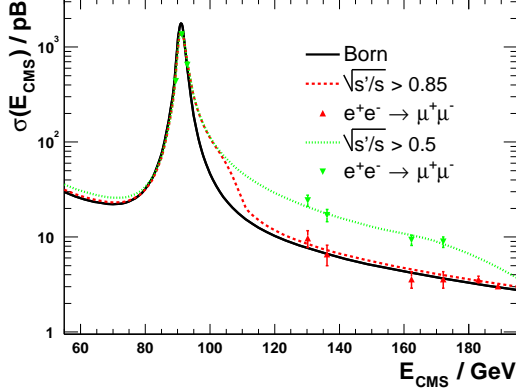


**Figure 1:** Energy dependence of the cross section  $\sigma$  at energies above the  $Z_0$  boson mass in comparison with DELPHI data [6]. Two different cuts on  $s'$  are applied, including and excluding a radiative return to the  $Z^0$  pole.

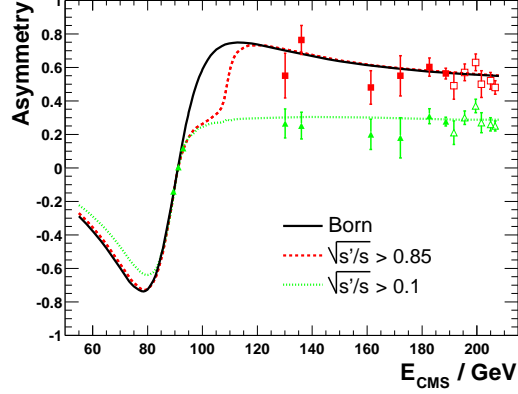


**Figure 2:** Forward-backward asymmetry above the resonance of the  $Z_0$  boson in comparison with combined muon and tau pair data from OPAL [7]. Again, different cuts on the effective c.m. energy  $\sqrt{s'}$  are plotted together with the Born expectation (without ISR). The open symbols mark preliminary data [8].

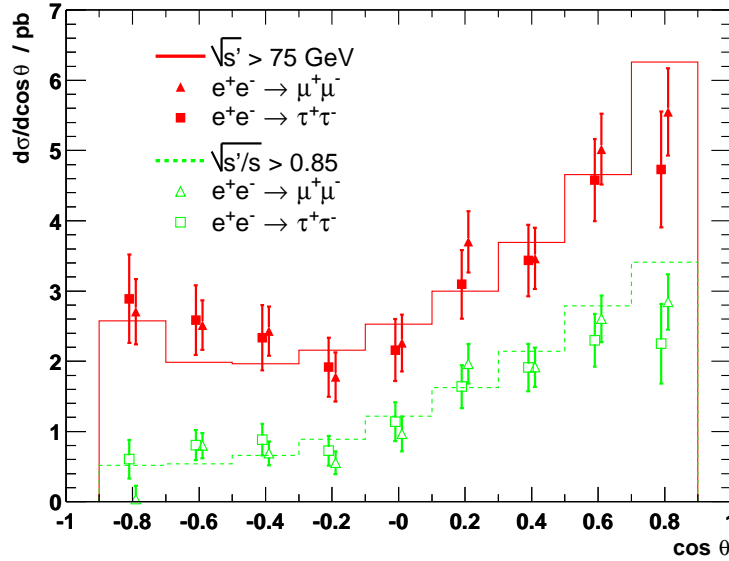


**Figure 3:** Differential cross section at  $\sqrt{s} = 189$  GeV in comparison with L3 data [9]. Different  $s'$  cuts have been applied.

In Figs. 4 and 5 the distribution of the effective c.m. energy  $\sqrt{s'}$  of the  $\mu^+\mu^-$  pair and the

distribution of photon energies are shown in comparison with results from KoralZ (second order). We find remarkably good agreement over almost the whole energy range in the  $\sqrt{s'}$  distribution. The energy distribution is dominated by the contribution of the hardest photon which is equally well described. The huge peak at 72.5 GeV corresponds to the radiation of one photon to reach the  $Z$ -resonance. Similarly, the edges at 48.9 GeV and 36.25 GeV correspond to a  $Z$  return via emissions of two hard photons. In this region our result differs slightly from KoralZ, since the interference effects become more pronounced. However, since the first order matrix element is used for the correction of every explicitly generated photon (not only the hardest) some of the higher order matrix element effects are already included. Note that we have concentrated on ISR effects only and therefore switched off FSR and weak corrections in KoralZ. In case only the first order correction of KoralZ is used, the results would be nearly indistinguishable.

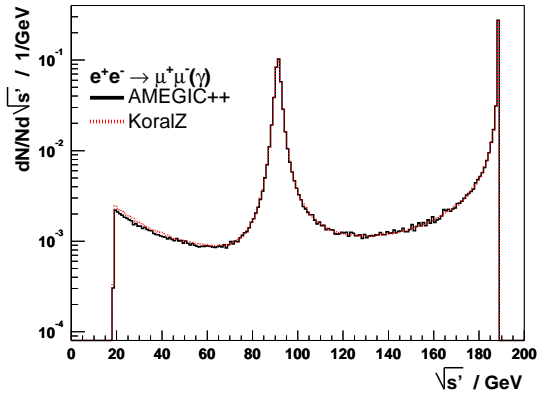


**Figure 4:** Distribution of the effective c.m. energy  $\sqrt{s'}$  of muon pairs at a beam energy of  $\sqrt{s} = 189$  GeV. First order results by AMEGIC++ are compared with the second order result of KoralZ.

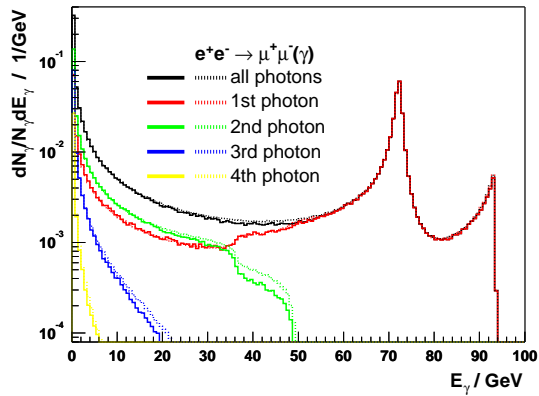


**Figure 5:** Energy distribution of ISR photons in comparison with KoralZ. The photons are ordered by their energies. Again, solid lines are results produced by AMEGIC++, dotted lines are results from KoralZ.

## Muon Collider

As another application we consider a possible muon collider [10]. Its main purpose will be the precise measurement of the properties of the Higgs boson once it is found. The muons are used for two reasons: First, lepton colliders provide comparably pure initial states allowing for spectroscopical measurements (like for instance the exact determination of branching ratios of rare decays like  $h \rightarrow \gamma\gamma$ ). Second, muons have a non-negligible coupling to the Higgs boson which in turn will be produced as an  $s$ -channel resonance. In Fig. 6 and Fig. 7 the total cross section and the forward-backward asymmetry for  $\mu^+\mu^- \rightarrow b\bar{b}$  are plotted with and without ISR effects assuming a Standard Model Higgs boson with a mass of 115 GeV. The small width of roughly 4 MeV is an experimental challenge, e.g. effects of beam resolution have to be considered. The main effect of ISR is to increase the background due to radiative return events to the  $Z^0$  peak. However, this background can be reduced via an appropriate  $s'$  cut. Of course, a radiative return to the

Higgs peak is also possible, but since the cross section is tiny the effect is small and only visible close to the peak.

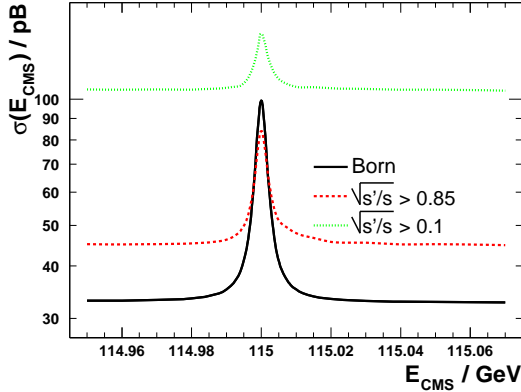


**Figure 6:** Energy dependence of the cross section  $\sigma$  around the resonance of the  $h_{\text{SM}}$  boson in the process  $\mu^+\mu^- \rightarrow b\bar{b}$ .

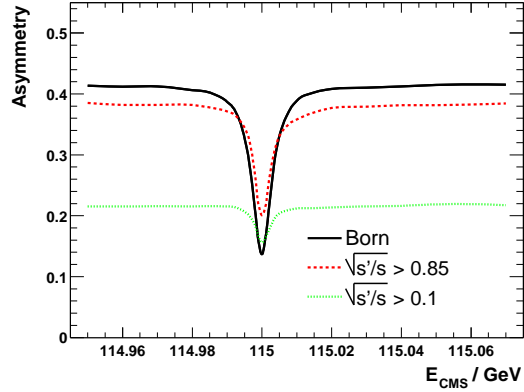


**Figure 7:** Forward-backward asymmetry around the resonance of the  $h_{\text{SM}}$  boson in the process  $\mu^+\mu^- \rightarrow b\bar{b}$ .

Since our method is general, we can discuss further the extension to any scalar boson propagating in the  $s$ -channel. As an example we consider the case of Higgs bosons in the Minimal Supersymmetric extension of the Standard Model (MSSM) [11, 12]. In this model there are two more neutral Higgs bosons which tend to be considerably heavier than the light one. For the following discussion let us constrain ourselves to a supergravity inspired supersymmetry breaking scenario [13, 16] with parameters to be found in the Appendix B. In this scenario we have a mass of  $m_{H_0} = 395.0$  GeV for the CP-even and a mass of  $m_{A_0} = 394.5$  GeV for the CP-odd Higgs boson. The total cross section can be found in Fig. 8 and the influence on the forward-backward asymmetry is given in Fig. 9. At this point in the mSUGRA parameter space the individual peaks can not be resolved and the two Higgs bosons appear as one single, comparably broad, resonance only. The effect of ISR is a slight shift of the peak to larger c.m. energies and an increase of background due to radiative return to the lower lying  $Z$  boson resonance. However, the latter effect can again be reduced by a suitable cut on the effective c.m. energy  $s'$ .

In striking contrast to the case of the lighter SM Higgs boson, in this case the radiative return to the peak structure from higher energies is important, see Figs. 10 and 11. Note that the contribution of a photon, a  $Z^0$  boson, and all three Higgs bosons propagating in the  $s$ -channel as well as all interference terms have been taken into account. The effect of the interplay of the different terms becomes apparent in angular distributions, cf. Fig. 12, where different cuts on the c.m. energy have been applied. The Born term is dominated by the off-peak  $Z$  boson contribution and exhibits therefore a slight angular dependence. When taking the radiative return to the heavy Higgs bosons peak into account, the distribution is only shifted due to the angular blind scalar coupling structure. The predominating contribution of the return to the  $Z$  resonance restores the angular distribution already known from Fig. 3.

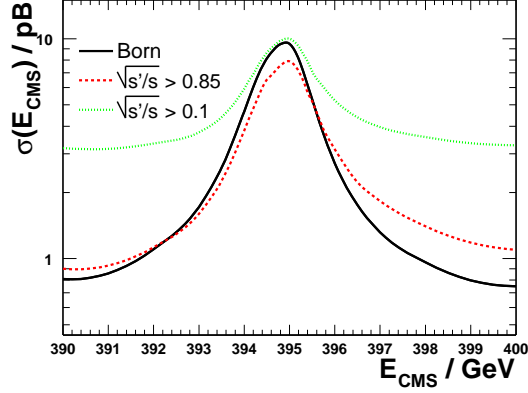


**Figure 8:** Energy dependence of the cross section  $\sigma$  around the resonance of the heavy scalar Higgs boson  $H_0$  and the pseudo scalar Higgs boson  $A_0$  in the process  $\mu^+\mu^- \rightarrow b\bar{b}$  for different  $s'$  cuts, as well as without ISR.

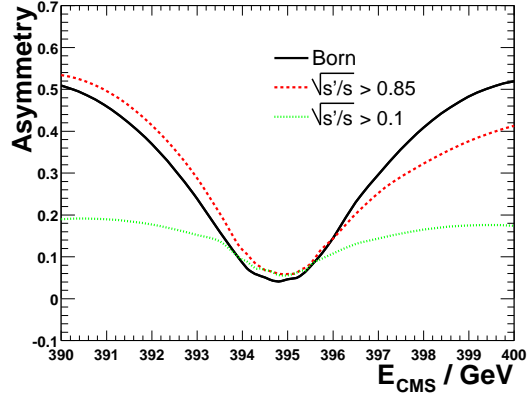


**Figure 9:** Asymmetry around the resonance of the heavy scalar Higgs boson  $H_0$  and the pseudo scalar Higgs boson  $A_0$  with and without ISR.

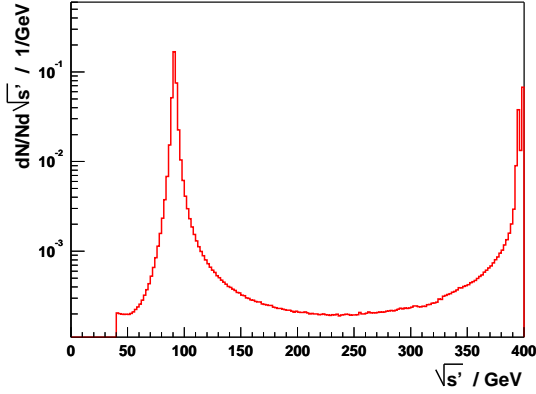


**Figure 10:** Distribution of the effective c.m. energy  $\sqrt{s'}$  for the process  $\mu^+\mu^- \rightarrow b\bar{b}$  at a beam energy of  $E_{\text{CMS}}=400$  GeV.

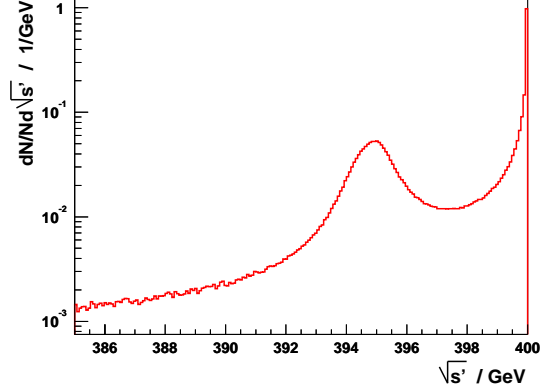


**Figure 11:** Detail of Fig. 10.

## 5. Conclusion and Outlook

In this paper we presented an implementation of the successful YFS algorithm into the matrix element generator AMEGIC++. To make full use of the possibilities offered by automatic matrix element generation with help of the helicity method and fully automatic integration of the matrix element we developed a new method to deal with the first order matrix element correction to multi photon emissions. We proved the quality of our method by two examples:

1. For lepton pair production at energies at and above the  $Z$  boson resonance, we have confronted our simulator with experimental data from the LEP experiment and another ISR generator, KoralZ. In both cases we found encouraging agreement.

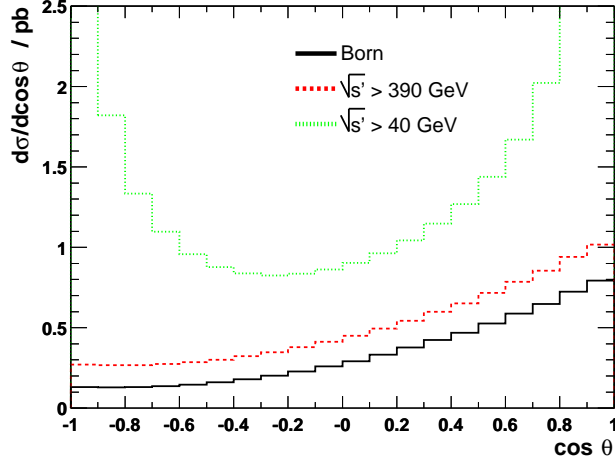


**Figure 12:** Angular distribution of the b-quark with respect to the incoming muon. Different cuts applied on  $\sqrt{s'}$  in order to include return events to the  $Z^0$  or to the heavy Higgs bosons  $H_0$  and  $A_0$  only. For comparison the Born expectation is plotted too.

2. The application of our approach to the  $s$ -channel production of Higgs bosons at a muon collider has illustrated the generality of our approach. Let us note that extensions to other bosons in the  $s$ -channel with other couplings is straightforward and will be addressed in the near future.
3. Furthermore, the interface of AMEGIC++ with the parton shower implemented in APACIC++ [14] provides a powerful tool for the simulation of hadronic final states including the effect of both ISR and the final state parton shower.

We feel obliged to comment briefly on possible improvements:

- Definitely, effects of Final State Radiation and its interference with ISR are missing and should be implemented. Additionally, some types of one-loop corrections like QCD corrections in the final state, electroweak corrections or box diagrams have not been implemented yet <sup>1</sup>. Also, an extension to second order corrections should be done to achieve the precision needed for a proper interpretation of the anticipated precision data.
- Apart from  $s$ -channel processes, at  $e^+e^-$  colliders processes like  $ZZ$  production play a crucial role and deserve a similar treatment. In the case of for instance  $WW$  production an extension of our method is not a trivial task.

---

<sup>1</sup>During the time of writing we became aware of [15], where an ISR calculation for a Higgs boson production at a muon collider was considered. This was based on the structure function approach and already includes FSR, IF-interference and QCD effects. Their findings are consistent with our Monte Carlo results.

## Acknowledgements

We would like to thank K. Hamacher, U. Flammeyer, U. Müller, A. Behrmann from the Delphi collaboration and P. Ward and D. Ward from the Opal collaboration for pleasant conversation and great help with the experimental data. F.K. gratefully acknowledges financial help of the DAAD. Furthermore, A.S. thanks BMBF for funding.

This work was supported in part by EU Fourth Framework Programme “Training and Mobility of Researchers”, Network “Quantum Chromodynamics and the Deep Structure of Elementary Particles”, contract FMRX-CT98-0194 (DG 12 - MIHT).

## A. The MC algorithm

In this appendix we would like to discuss the Monte Carlo procedure for the generation of ISR photons, further details of the first three steps can be found in [3].

### 1. Choice of the reduced c.m. energy squared

First, the reduced c.m. energy squared is determined. This is done according to a “crude distribution” that consists of a fast approximation for the energy dependence of the cross section. This approximation already exhibits the correct peak structure as given by the  $s$ -channel propagators. Additionally, it includes the leading logarithmic photon factor. The corresponding probability density in terms of the energy fraction  $\nu = 1 - s'/s$  reads

$$f(\nu) = \frac{\gamma}{(1-\nu)\nu^{1-\gamma}} \Psi(\nu) \quad (\text{A.1})$$

with

$$\Psi(\nu) = (1-\nu) \sigma_{\text{Born}}(s') \hat{\mathcal{J}}(\nu) \quad \text{and} \quad \gamma = \frac{2\alpha}{\pi} \left( \ln \frac{s}{m^2} - 1 \right) \ln \varepsilon. \quad (\text{A.2})$$

The energy fraction  $\nu$  can be determined according to  $f(\nu)$  by standard Monte Carlo sampling techniques. In the equation above  $\hat{\mathcal{J}}(\nu)$  is an approximate form of the Jacobian that will be discussed in step 3(b).

### 2. Choice of number of resolvable photons

Having determined the effective center of mass energy squared  $s' = s(1-\nu)$ , we proceed by choosing the number of resolvable photons which in turn have to be generated explicitly. In the logarithmic approximation the photon number  $N_\gamma$  follows a shifted Poisson distribution:

$$f(N_\gamma - 1) = e^{-\mu} \frac{\mu^{N_\gamma - 1}}{(N_\gamma - 1)!}. \quad (\text{A.3})$$

Obviously, its mean value depends on both  $s'$  and the photon resolution parameter  $\varepsilon$ . It is given by

$$\mu = \int \frac{d^3 \vec{k}}{k^0} \tilde{S}(p_1, p_2, k) \Theta \left( \frac{2k^0}{\sqrt{s}} - \varepsilon \right) \Theta \left( \nu - \frac{2k^0}{\sqrt{s}} \right) \quad (\text{A.4})$$

$$= \frac{2\alpha}{\pi} \ln \left( \frac{s}{m_e^2} \right) \ln \left( \frac{\nu}{\varepsilon} \right) \Theta(\nu - \varepsilon). \quad (\text{A.5})$$



This can be identified in the master formula, Eq.(2.5), considering the additional constraint on the photon energies (the second  $\Theta$ -function) not to exceed  $s'$ .

### 3. Construction of four-momenta

The construction of four-momenta for the photons is achieved in two steps:

- (a) **Angles:** The photon angles are now individually appointed to each photon with the help of the eikonal  $\tilde{S}$ . Clearly,  $\tilde{S}$  exhibits no dependence on the azimuthal angle  $\varphi$ , hence this angle is distributed uniformly. In contrast,  $\tilde{S}$  depends strongly on the polar angle  $\vartheta$ , which in turn is chosen according to

$$\bar{f}(\cos \vartheta) = \frac{1}{(1 - \beta \cos \vartheta)(1 + \beta \cos \vartheta)} \quad \text{with} \quad \beta = \sqrt{1 - \frac{4m^2}{s}}. \quad (\text{A.6})$$

Note that terms proportional to the lepton mass have been discarded at this stage. Therefore, a correction weight is introduced for each photon

$$w_{\text{angle}}(\vartheta) = \frac{f(\vartheta)}{\bar{f}(\vartheta)}, \quad (\text{A.7})$$

where the exact distribution  $f(\vartheta)$  is given by

$$f(\vartheta) = \bar{f}(\cos \vartheta) - \frac{m^2}{s - 2m^2} \left( \frac{1}{(1 - \beta \cos \vartheta)^2} + \frac{1}{(1 + \beta \cos \vartheta)^2} \right). \quad (\text{A.8})$$

Thus, the weight to reproduce the correct mass-dependence reads

$$w_{\text{mass}} = \prod_{i=1}^{N_\gamma} w_{\text{angle}}(\vartheta_i). \quad (\text{A.9})$$

- (b) **Energies:** The next step is the assignment of energies to each of the photons. In case that exactly one photon above the threshold has been generated, the energy of this photon is already completely constrained by  $\nu$  and the chosen photon angles due to overall four-momentum conservation. In the case that more than one photon have been generated, the additional photon energies are chosen according to  $dk^0/k^0$ , i.e. the eikonal  $\tilde{S}$ . Then a scaling of all photons is performed in order to achieve four-momentum conservation. Thereby an Jacobian

$$\mathcal{J}(K, \nu) = \frac{1}{2} \left( 1 + \frac{1}{\sqrt{1 - A\nu}} \right) \quad (\text{A.10})$$

with the abbreviations

$$A = \frac{K^2 P^2}{(KP)^2}, \quad K = \sum_{n=1}^{N_\gamma} k_n \quad (\text{A.11})$$

is introduced. It had been taken into account already in step 1 as  $\hat{\mathcal{J}}$  assuming  $A = 1$ , since the photon momenta have not been known at this time. A correction weight

$$w_{\text{jac}} = \frac{\mathcal{J}(K, \nu)}{\hat{\mathcal{J}}(\nu)} \quad (\text{A.12})$$

is introduced to cure this simplification. Furthermore, all photon energies have to be above the limit  $\varepsilon\sqrt{s}/2$  after rescaling, in order to avoid double counting. This leads to an additional weight

$$w_\varepsilon = \Theta\left(k_n^0 - \frac{\sqrt{s}}{2}\varepsilon\right). \quad (\text{A.13})$$

#### 4. Matrix element correction

The next step is the calculation of the matrix element correction. This is done by introducing an additional weight according to

$$w_{\text{ME}} = \frac{1}{\sigma_0(s')} \left\{ \beta_0^{(1)}(p_i, q_j) + \sum_{n=1}^{N_\gamma} \frac{\beta_1^{(1)}(p_i, q_j, k_n)}{\tilde{S}(p_i, k_n)} \right\}. \quad (\text{A.14})$$

#### 5. Re-weighting

The last step is the calculation of the final weight in order to cure the approximations made during the choice of the reduced c.m. energy (step 1) and the determination of the photon momenta (step 3) as well as to incorporate the matrix element corrections

$$w_{\text{MC}} = w_{\text{mass}} w_{\text{jac}} w_\varepsilon w_{\text{ME}}. \quad (\text{A.15})$$

This weight can now be used in a rejection method to produce unweighted events.

The ISR simulation in **AMEGIC++** differs from this general description mainly in steps 1 and 4.

In step 1, a multichannel method is used to determine  $s'$  to incorporate complicated peak structures. It can therefore be understood as the first part of the multichannel determination of the final state momenta. A library of fast  $f\bar{f} \rightarrow f'\bar{f}'$  cross sections for arbitrary scalar and vector  $s$ -channel resonances enables the simulation of many processes in the SM and beyond. Due to the rejection mechanism these cross sections can be also used for multi-jet productions.

In step 4 the evaluation of the matrix element correction is modified as described in section 2, thereby taking full advantage of the features of **AMEGIC++**.

## B. Program Parameters

The parameters used for the calculation of results presented in section 4 are given in Tab. 1 and Tab. 2.

To include higher order effects in the Yukawa coupling we have used a running b-quark mass according to the well known relation

$$m_\mu = m_{\mu_0} \left( \frac{\alpha_s(\mu)}{\alpha_s\mu_0} \right)^{\frac{\gamma_{m,0}}{\beta_0}} \quad (\text{B.1})$$

with

$$\gamma_{m,0} = 1, \quad \beta_0 = \frac{1}{12}(33 - 2n_f). \quad (\text{B.2})$$

$\alpha_{\text{QED}}$	1./137.035995
$\sin^2 \vartheta_w$	0.23117
$M_Z$	91.1882 GeV
$\Gamma_Z$	2.4952 GeV
$m_b$	5.0 GeV
$m_c$	1.3 GeV
$m_\mu$	105.658 MeV
$m_\tau$	1.777 GeV
$v$	246.2 GeV
$m_{h_{sm}}$	115.0 GeV
$\Gamma_{h_{sm}}$	3.8 MeV

**Table 1:** Standard Model parameter used for the simulation.

$M_0$	100. GeV	$m_{H_0}$	395.0 GeV
$M_{1/2}$	250. GeV	$\Gamma_{H_0}$	1.07 GeV
$A_0$	-100. GeV	$m_{A_0}$	394.5 GeV
$\tan \beta$	10.	$\Gamma_{A_0}$	1.29 GeV
$\mu$	+1		
$m_t$	175. GeV		

**Table 2:** The mSugra point SPS1 according to [16] and the corresponding properties of the heavy Higgs bosons in the MSSM. The widths of the Higgs bosons have been calculated with AMEGIC++.

## References

- [1] D. R. Yennie, S. C. Frautschi, and H. Suura, *Ann. Phys.* **13** (1961), 379–452.
- [2] F. Krauss, R. Kuhn and G. Soff, *JHEP* **0202** (2002) 044
- [3] S. Jadach and B. F. L. Ward, *Comput. Phys. Commun.* **56** (1990), 351–384.
- [4] S. Jadach, B. F. Ward and Z. Was, *Comput. Phys. Commun.* **79** (1994) 503.
- [5] R. Kleiss and R. Pittau, *Comput. Phys. Commun.* **83** (1994) 141. F. A. Berends, R. Pittau and R. Kleiss, *Nucl. Phys. B* **424** (1994) 308.
- [6] P. Abreu *et al.* [DELPHI Collaboration], *Phys. Lett. B* **485** (2000) 45. P. Abreu *et al.* [DELPHI Collaboration], *Eur. Phys. J. C* **11** (1999) 383. P. Abreu *et al.* [DELPHI Collaboration], *Eur. Phys. J. C* **16** (2000) 371.
- [7] G. Abbiendi *et al.* [OPAL Collaboration], *Eur. Phys. J. C* **13** (2000) 553.
- [8] OPAL Collab., OPAL Physics Note PN469 (February 2001) and references therein.
- [9] M. Acciarri *et al.* [L3 Collaboration], *Phys. Lett. B* **479** (2000) 101.
- [10] C. M. Ankenbrandt *et al.*, *Phys. Rev. ST Accel. Beams* **2** (1999) 081001.
- [11] see for instance: H. E. Haber and G. L. Kane, *Phys. Rept.* **117** (1985) 75.
- [12] V. D. Barger, M. S. Berger, J. F. Gunion and T. Han, *Phys. Rept.* **286** (1997) 1.
- [13] see for instance: H. P. Nilles, *Phys. Rept.* **110** (1984) 1.
- [14] R. Kuhn, F. Krauss, B. Ivanyi and G. Soff, *Comput. Phys. Commun.* **134** (2001) 223.
- [15] S. Dittmaier and A. Kaiser, [hep-ph/0203120](#).
- [16] B. C. Allanach *et al.*, in *Proc. of the APS/DPF/DPB Summer Study on the Future of Particle Physics (Snowmass 2001)* ed. R. Davidson and C. Quigg.